



*Supplement of*

## **The 2020 European Seismic Hazard Model: overview and results**

**Laurentiu Danciu et al.**

*Correspondence to:* Laurentiu Danciu ([laurentiu.danciu@sed.ethz.ch](mailto:laurentiu.danciu@sed.ethz.ch))

The copyright of individual parts of the supplement might differ from the article licence.

In this supplementary materials section, we provide additional resources to explore the differences between the ESHM20 (Danciu et al 2021) and ESHM13 (Wössner et al 2013) models.

First, we present the percentage difference for PGA between ESHM20 and ESHM13 for the capital cities of Europe (Table S1). Next, we compare the total magnitude frequency distribution of the two models. Additionally, we provide spatial differences in earthquake rate forecasts between the two hazard models for magnitudes 5.5 and 6.5. Finally, we include a series of trellis plots to facilitate a comparative analysis of the ground motion characteristics models.

More supplementary materials and comparison plots are available online in the ESHM20's repository:

[https://gitlab.seismo.ethz.ch/efehr/eshm20/-/tree/master/additional\\_materials?ref\\_type=heads](https://gitlab.seismo.ethz.ch/efehr/eshm20/-/tree/master/additional_materials?ref_type=heads), (last access July 2024). This repository contains additional plots depicting regional variations in all source attributes for all source models. The comparisons include plots that compare hazard curves and hazard spectra between ESHM20 and ESHM13 for 420 cities across the Euro-Mediterranean region.

Figure S1 shows a comparison plot of magnitude frequency distributions (MFDs) between ESHM20 and ESHM13. The plot illustrates the cumulative annual activity rates versus moment magnitude ( $M_w$ ) for various individual MFD models from both regional hazard models. ESHM20 models are represented by continuous lines: ESHM20-Hybrid (active fault and background seismicity), ESHM20-ASM (area source model), ESHM20-Weighted (weighted ensemble rate model), and ESHM20-SEIS (background smoothed seismicity). ESHM13 models are shown with dotted lines: ESHM13-Weighted (weighted rate model), ESHM13-ASM (area source model), ESHM13-Hybrid (active fault and background seismicity), and ESHM13-SEIFA (smoothed seismicity model). Grey squares indicate observed cumulative earthquake rates from 100 to 2014, aggregated at the completeness *superzone* levels.

The ESHM20 rate models are generally more closely aligned with the observed data than the ESHM13 models. The ESHM20-Weighted model (black line), as well as ASM (orange line) exhibits a consistent fitting across the entire magnitude range. The differences on the magnitude range of  $M_w6$  to  $M_w7$  is due to the contribution of the active faults branch from the Hybrid model (green line). On the other hand, ESHM13 models show more significant deviations, particularly at higher magnitudes ( $M_w > 7.0$ ); as a result, the ESHM13-total weighted rate model (black dotted line) deviates significantly from the observed rates. It shall be noted, that the observed cumulative rate differences between the ESHM20 and ESHM13 models can be attributed to a variety of factors, including spatial extent and source harmonization, as well as the calibration of the active fault information. The noticeable difference between the two hybrid earthquake rate forecasts, which incorporate the earthquake rate forecast of active faults, underscores the impact of updated fault database and refined methodologies in ESHM20.

Furthermore, to investigate these changes the *ensemble* earthquake rate forecast of the ESHM20 minus that of ESHM13 are compared at each grid site for two magnitudes,  $M_w > 5.5$  in Figure S2 and  $M_w > 6.5$  in Figure S3, respectively. Changes in the seismogenic sources cause many of the local differences across the entire region. Regional discrepancies in the earthquake rates are likely caused by the new earthquake catalogue, new

completeness time-magnitude intervals, new magnitude frequency distributions (Pareto Tapered Distribution and exponential GR distribution), updated slip-rates and maximum magnitude of the faults, new adaptive-smoothing technique, new subduction sources, new logic tree and its implementation.

In addition to the earthquake rate forecast maps, we have also included four figures that facilitate a detailed comparison of the ground motion models between ESHM20 and ESHM13. These figures illustrate acceleration response spectra for various earthquake scenarios, for comparison purposes. Specifically, Figure S4 focuses on active shallow crust scenarios, Figure S5 shows the subduction interface scenarios, Figure S6 addresses the comparison for subduction in-slab, and finally, in Figure S7 the comparison for craton regions is shown. These trellis plots provide a comprehensive view of how ground motion models differ between ESHM20 and ESHM13, aiding in the understanding of seismic hazard variations across these two regional models.

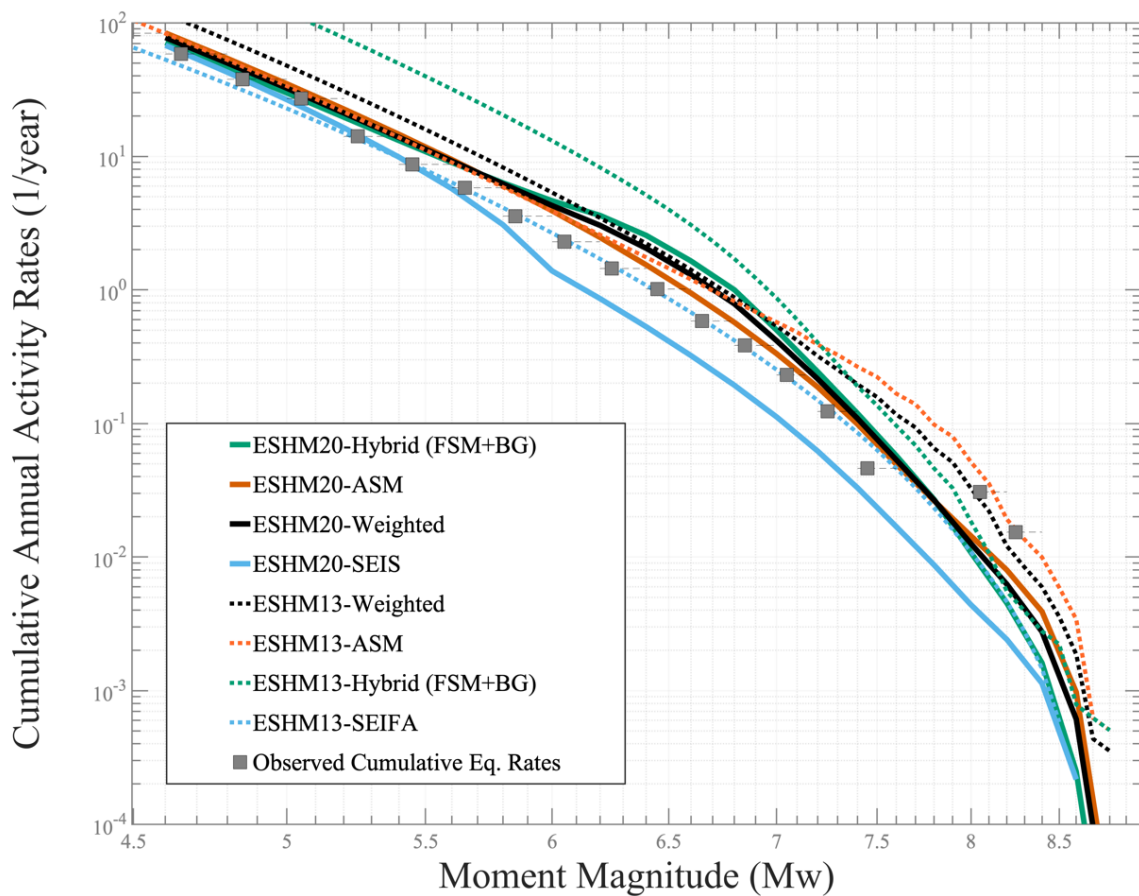
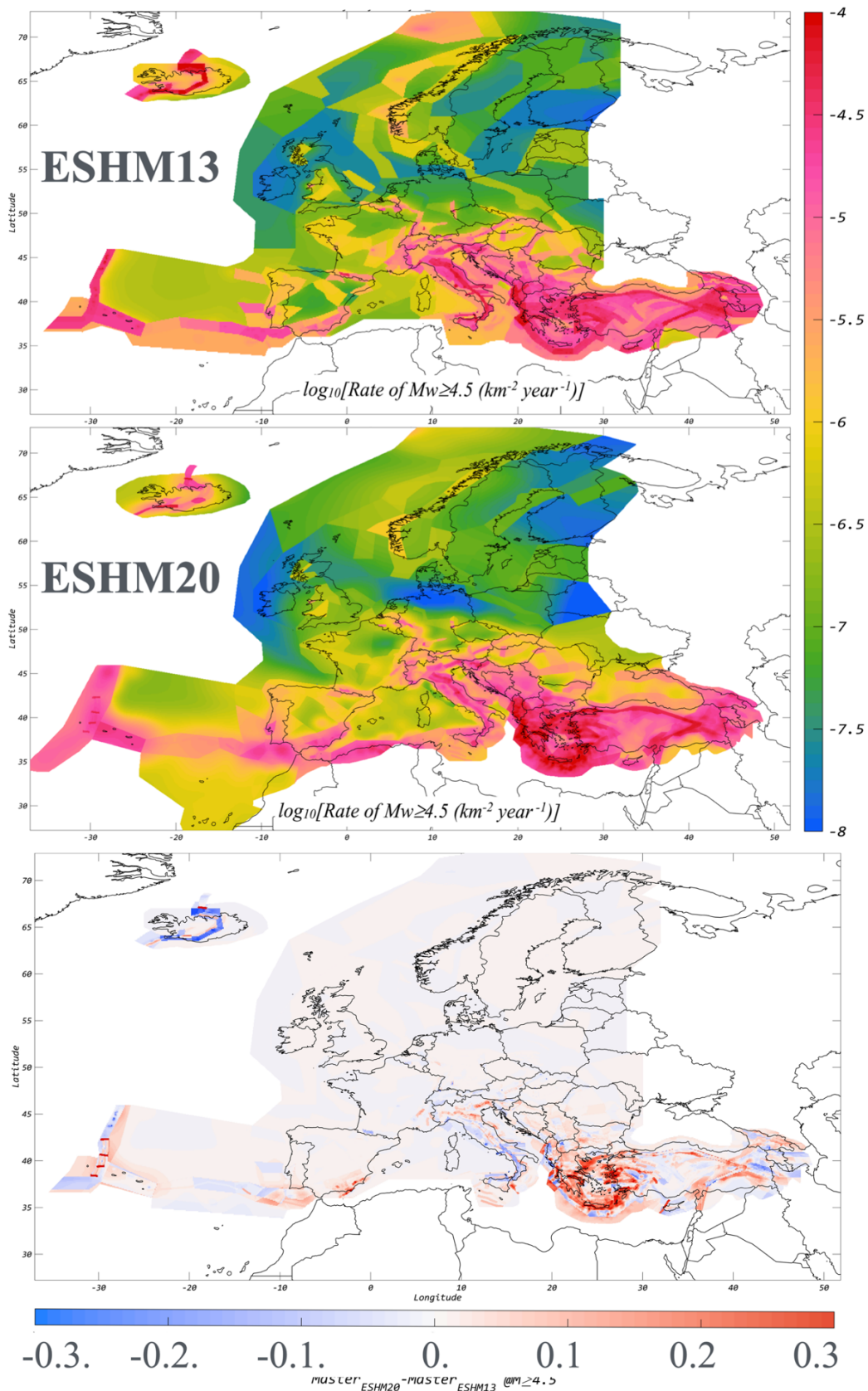


Figure S1: Annual earthquake rate forecasts for both ESHM13 (top panel) and ESHM20 (mid panel) ensemble models specifically for  $M_w \geq 5.5$ . Difference rate maps, represented as ESHM20 - ESHM13 (bottom panel)



### ESHM20<sup>Norm</sup> - ESHM13<sup>Norm</sup>. @M<sub>w</sub> >= 5.5

Figure S2: Annual earthquake rate forecasts for both ESHM13 (top panel) and ESHM20 (mid panel) ensemble models specifically for  $M_w \geq 5.5$ . Difference rate maps, represented as ESHM20 - ESHM13 (bottom panel)

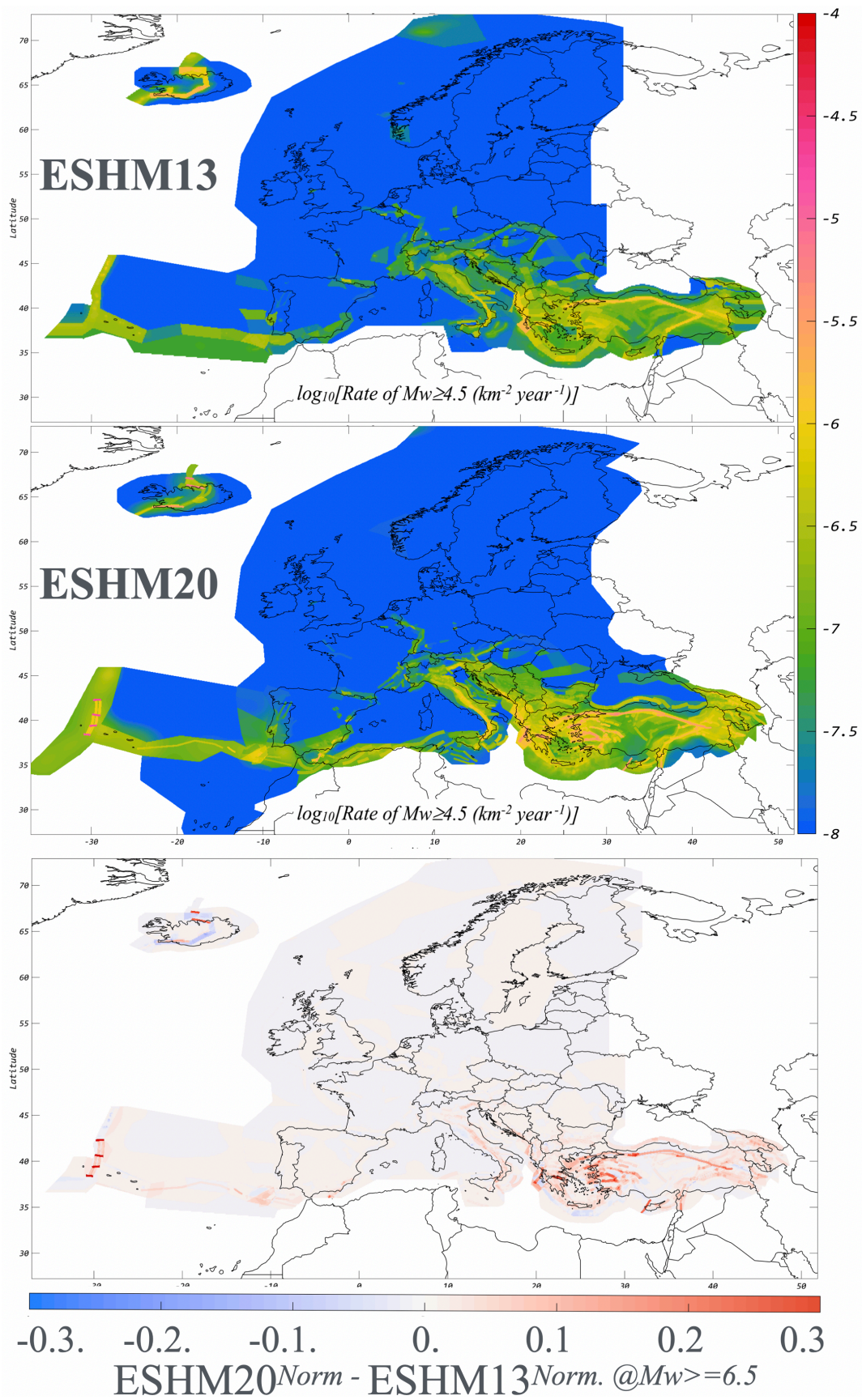


Figure S3: Annual earthquake rate forecasts for both ESHM13 (top panel) and ESHM20 (mid panel) ensemble models specifically for  $M_w \geq 6.5$ . Difference rate maps, represented as ESHM20 - ESHM13 (bottom panel)

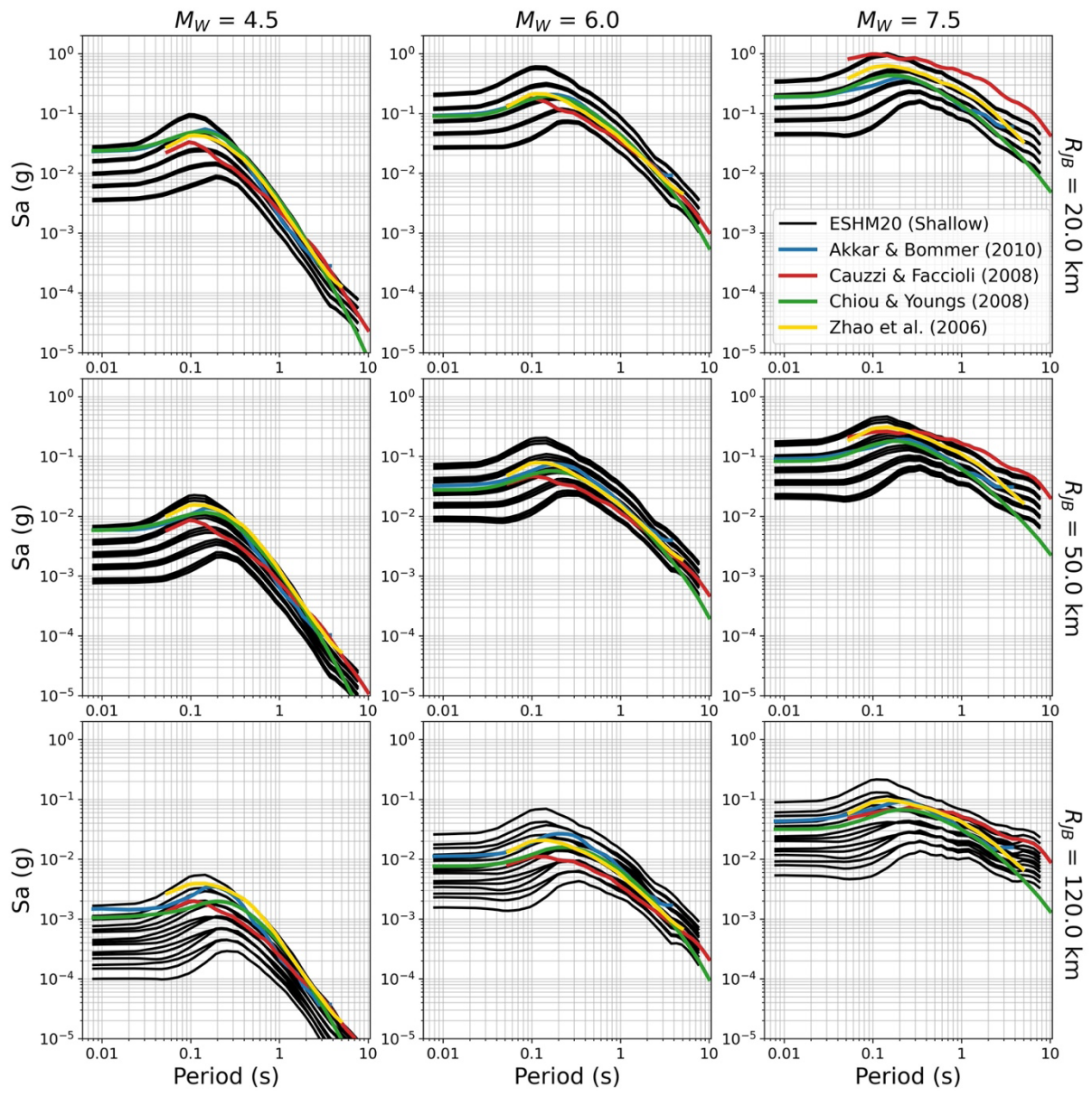


Figure S4: Trellis plots comparing the response spectra of the nine-branch default shallow logic tree against the ESHM13 shallow crust GMPE selection Delavaud et al. (2012) for a strike-slip earthquake and sites located at 20, 50 and 120 respectively, assuming a measured site condition of VS30 800 m/s

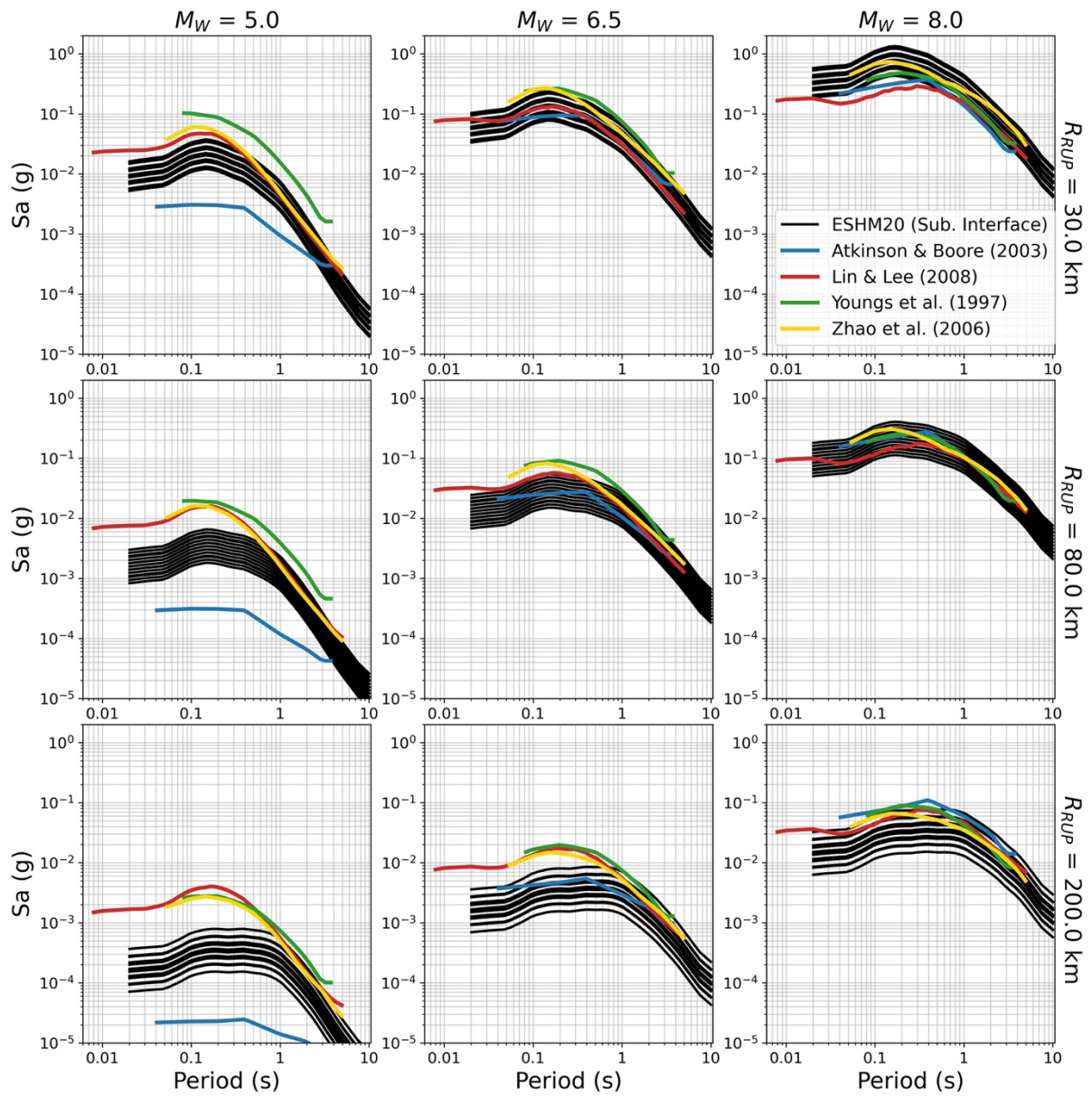


Figure S5: Trellis plots comparing the response spectra of the subduction interface logic tree against the ESHM13 GMPE used to model the subduction interface, for sites located at  $R_{rup}=30, 80$  and  $200$ km assuming a measured site condition of VS30 800 m/s

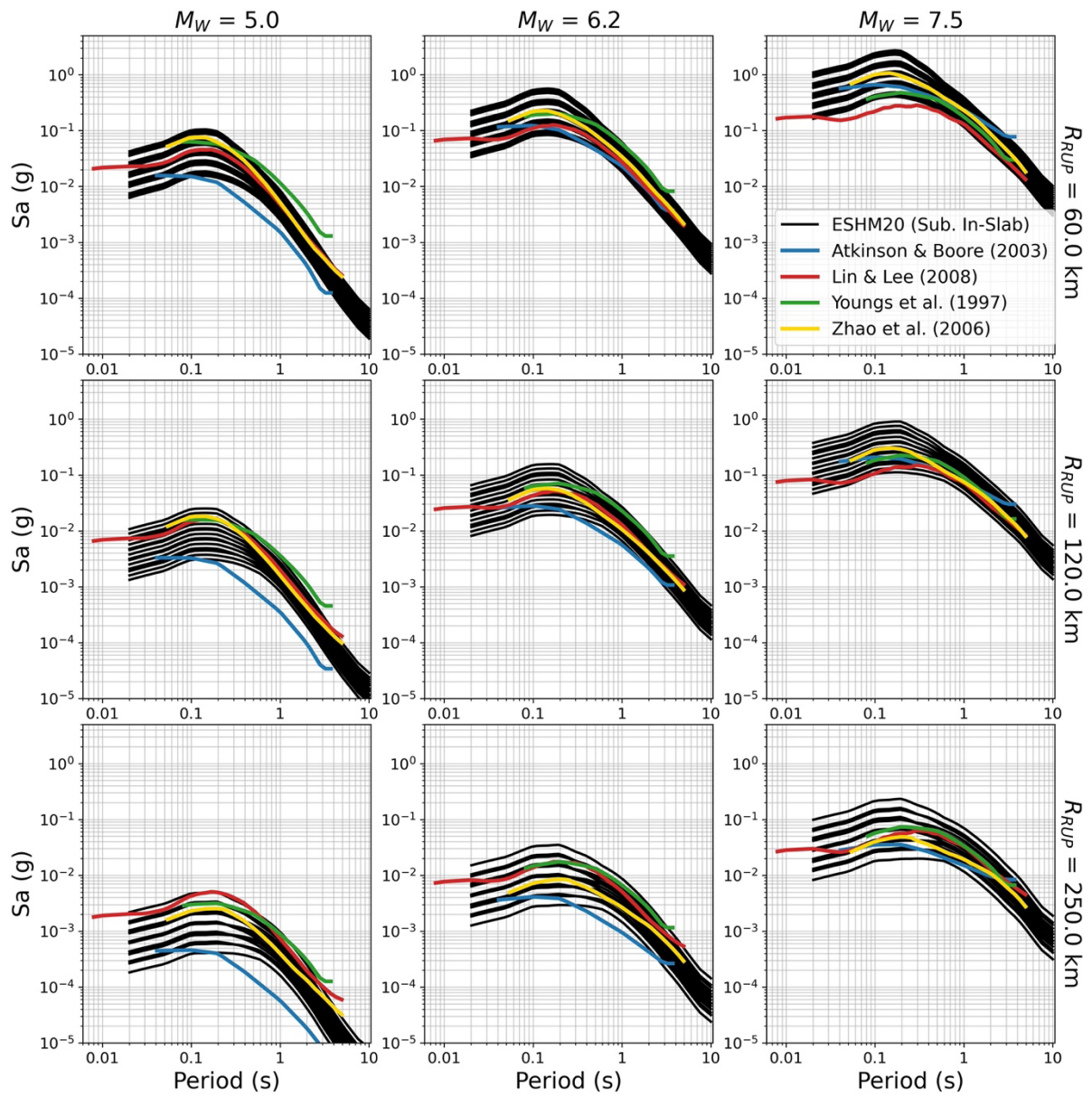


Figure S6: Trellis plots comparing the response spectra of the subduction in-slab logic tree against the ESHM13 GMPE used to model the subduction in-slab, for sites located at  $R_{rup}=60, 120$  and  $250$ km assuming a measured site condition of VS30 800 m/s



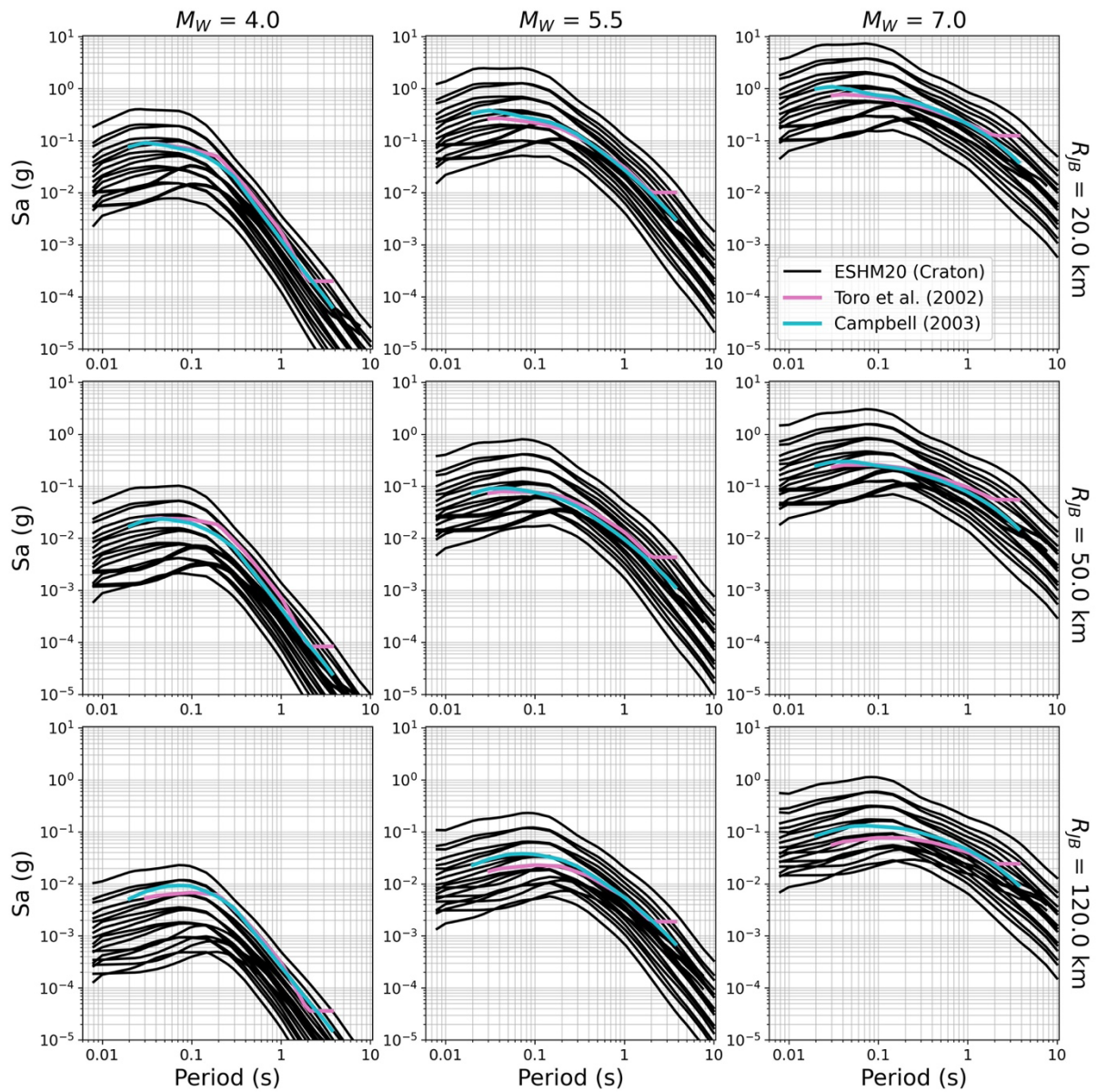


Figure S7: Trellis plots comparing the response spectra of the ESHM20 logic tree against the ESHM13 GMPE selection Delavaud et al. (2012) for craton regions, sites located at 20, 50 and 120Km, respectively, assuming a measured site condition of VS30 800 m/s

To conclude, it is important to note that ESHM20 has been established as the successor to ESHM13 and is now the recommended reference for seismic hazard assessment in Euro-Mediterranean region. Given the substantial improvements and updates incorporated into ESHM20, we strongly advocate for its adoption as the preferred choice for seismic hazard analysis in the region.

Table S1: Percentage Difference [%] in PGA Values for APE 1/475years between ESHM20 and ESHM13 for European Capital Cities

<b>capital</b>	<b>lat</b>	<b>lon</b>	<b>ESHM20 PGA(g) APE 1/475yrs</b>	<b>ESHM13 PGA(g) APE 1/475yrs</b>	<b>Percentage difference (ESHM20- ESHM13)/ESHM13 [%]</b>
Amsterdam	52.35	4.9166	0.0097	0.0188	-48.40
Andorra	42.5	1.5165	0.0575	0.087	-33.91
Athens	37.9833	23.7333	0.2273	0.3181	-28.54
Belgrade	44.8186	20.468	0.1111	0.1028	8.07
Berlin	52.5218	13.4015	0.001	0.0089	-88.76
Bern	46.9167	7.467	0.0567	0.1065	-46.76
Bratislava	48.15	17.117	0.074	0.1117	-33.75
Brussels	50.8333	4.3333	0.0312	0.0731	-57.32
Bucharest	44.4334	26.0999	0.3137	0.2255	39.11
Budapest	47.5	19.0833	0.0596	0.0781	-23.69
Chisinau	47.005	28.8577	0.1486	0.1559	-4.68
Copenhagen	55.6786	12.5635	0.0043	0.024	-82.08
Dublin	53.3331	-6.2489	0.0031	0.008	-61.25
Helsinki	60.1756	24.9341	0.0049	0.008	-38.75
Istanbul	41.0151	28.9795	0.3873	0.4176	-7.26
Lisbon	38.7227	-9.1449	0.1339	0.2415	-44.55
Ljubljana	46.0553	14.515	0.2794	0.2345	19.15
London	51.5072	-0.1275	0.0045	0.0129	-65.12
Luxembourg	49.6117	6.13	0.0184	0.0303	-39.27
Madrid	40.4	-3.6834	0.0107	0.013	-17.69
Monaco	43.7396	7.4069	0.123	0.1558	-21.05
Nicosia	35.1667	33.3666	0.2044	0.2551	-19.87
Oslo	59.9167	10.75	0.0119	0.0184	-35.33
Paris	48.8667	2.3333	0.0039	0.0144	-72.92
Podgorica	42.466	19.2663	0.1734	0.2416	-28.23
Prague	50.0833	14.466	0.0062	0.0139	-55.4
Reykjavik	64.15	-21.95	0.1467	0.3629	-59.58
Riga	56.95	24.1	0.0126	0.0228	-44.74

Rome	41.896	12.4833	0.0904	0.1894	-52.27
San Marino	43.9172	12.4667	0.1786	0.2463	-27.49
Sarajevo	43.85	18.383	0.1299	0.1215	6.91
Skopje	42	21.4335	0.1973	0.249	-20.76
Sofia	42.6833	23.3167	0.2622	0.282	-7.02
Stockholm	59.3508	18.0973	0.0107	0.005	114
Tallinn	59.4339	24.728	0.008	0.0156	-48.72
Tirana	41.3275	19.8189	0.3741	0.3766	-0.66
Vaduz	47.1337	9.5167	0.0681	0.1269	-46.34
Valletta	35.8997	14.5147	0.0531	0.0644	-17.55
Vienna	48.2	16.3666	0.0708	0.1079	-34.38
Vilnius	54.6834	25.3166	0.0043	0.0077	-44.16
Warsaw	52.25	21	0.0036	0.0146	-75.34
Zagreb	45.8	16	0.2454	0.2421	1.36